Variable Dynamic Testbed Vehicle: Dynamics Analysis

Allan Y. Lee*
M.S. 198-235
Jet Propulsion laboratory
California institute of Technology
Pasadena, California 91109-8099
(818)-354-4097

Nhan T. Le
University of California
Los Angeles, California

Alan T. Marriott
Jet Propulsion Laboratory
Pasadena, California

Abstract

The Variable Dynamic Testbed Vehicle (VDTV) concept has been proposed as a tool to evaluate collision avoidance systems and to perform driving-redated human factors research. The goal of this study is to analytically investigate to what extent a VDTV with adjustable front and rear anti-roll bar stiffnesses, programmable damping rates, and four-wheel-steering can emulate the lateral dynamics of a broad range of passenger vehicles. Using a selected compact-sized automobile as a baseline, our study indicated this baseline vehicle can be controlled to emulate the lateral response characteristics (including the vehicle's understeer coefficient and the 90% lateral acceleration rise time in a J-turn maneuver) of a fleet of production vehicles, from low to high lateral acceleration conditions. Also, the roll gradient of the baselined vehicle can be altered via changes made to the torsional stiffnesses of the front and/or rear anti-roll bars to emulate the roll stiffnesses of a fleet of production vehicles.

Introduction

To study the correlation between vehicle response characteristics and driver commands relative to crash avoidance, the National Highway Traffic Safety Administration's Office of Crash Avoidance Research (OCAR) has at its disposal a comprehensive set of tools and facilities. These include the Vehicle Research and Test Center, and the (currently being developed) National Advanced Driving Simulator. To augment these tools and facilities, OCAR has defined its concept of a Variable Dynamic Testbed Vehicle (VDTV).[1] This vehicle will be capable of emulating a broad range of automobile dynamic characteristics, allowing it to be used in development of collision avoidance systems, and conducting of driving-related human factors research, among other applications.

Vehicles with "programmable" response characteristics have been proposed and developed in the past. In the 1970's, an experimental vehicle, called Variable Response Vehicle, was developed by the General Motors Corporation for vehicle handling research.[2] It had independent electro-hydraulic controlled front and rear steering actuators and a front steering feel system. These active systems enabled it to emulate a variety of directional control characteristics. In the 1990's, a similar research vehicle, called Simulator Vehicle, was developed by the Nissan Motor Company.[3] Both yaw rate and lateral acceleration response characteristics of this vehicle were varied independently. It was used to study the relation between driver's perception and vehicle handling quality.

To emulate both the lateral and longitudinal response characteristics of a broad range of vehicles, the "mechanical" steering, suspension, and braking sub-systems of a "(passive" vehicle must

* To whom all correspondence should be sent

all be made "programmable". With regard to emulating the lateral response characteristics of vehicles, an earlier study[4] indicated that the VDTV must have the following active sub-systems: (1) steering: steer-by-wire, programmable steering feel as well as four-wheel-steering, and (2) suspension: semi-active suspension as well as variable front and rear anti-roll bar systems. other active sub-systems considered in Reference 4 (such as the brake-by-wire and throttle-by-wire systems) were not included in this study.

Equipped with the above mentioned actively controlled systems, the lateral response characteristics of the VDTV can be conveniently altered via the governing control algorithms. However, it was not clear what range of production vehicles could be emulated by such a variable dynamic vehicle. One objective of the dynamics analysis was to gain a quantitative understanding of the "emulability" of such a variable dynamic vehicle. The second objective was to generate quantitative information for the functional requirements document[14] that accompanied the VDTV Request for Proposal.

Scope and Approach of Dynamics Analysis

The scope and approach taken in the dynamics analysis are as follows:

1. A vehicle dynamics simulation program, called Vehicle Dynamic Analysis, Nonlinear (VDANL) was selected as the simulation tool to perform all the vehicle dynamic computations.

2. The VDANL program has parameter files for about twenty passenger vehicle models. Only five models were selected to represent a broad range of production passenger vehicles.

3. Three performance metrics were selected to characterize both the steady-state and transient lateral responses of these production vehicle models in "representative" cornering maneuvers.

4. One of the five models studied was selected as the baseline VDTV. However, to account for the added weights of the data acquisition system, four-wheel-steering system, etc., several vehicle and tire parameters of the selected vehicle model were modified accordingly.

5. Two sensitivity analyses were made to assess to what degree vehicle performance metrics selected in step (3) are influenced by the following vehicle parameters: (a) the torsional stiffnessess of the front and rear anti-roll bars, and (b) the damping rates of the suspension shock absorbers.

6. A simulation study was made to assess to what extent the understeer coefficient and speed of lateral response of the five production vehicles selected in step (2) can be emulated by a four-wheel-steered VDTV.

7. The Consumers Union obstacle avoidance course (to be described latter) was used to objectively evaluate the handling qualities of passenger vehicles during emergency double lane change maneuvers. The performance of the baseline VDTV in making double lane change maneuvers using different combinations of tires and four wheel steering control algorithm were compared.

Results obtained from these seven steps are given in the following sub-sections.

Vehicle Dynamics Simulation Program

A vehicle dynamics simulation program, developed by Systems Technology, Incorporated, called "Variable Dynamics Analysis, Non-Linear" (VDANL) was used in this research. This program was originally developed to study the performance of vehicle/driver systems in a variety of driving scenarios and conditions, and to study vehicle lateral control and stability.[5]

A signal flow diagram of the program VDANL is depicted in Figure 1 (from Reference 6). The program VDANL has a total of seventeen degrees-of-freedom (DOF's). The block labeled "Vehicle Dynamics" (in Figure 1) has six DOF's for the sprung mass and two DOF's each for the front and rear unsprung masses. In the block

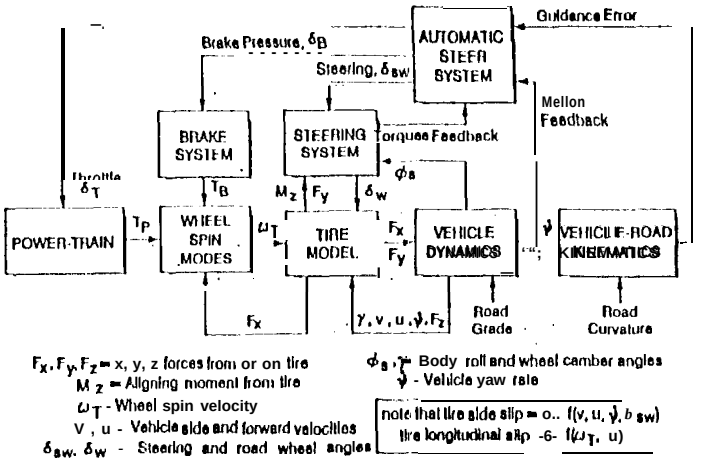

Figure 1: Flow diagram of the VDANL vehicle dynamic simulation program

labeled "Tire Dynamics," four DOFs for the rotational speeds of the four wheels are included. Finally, one degree of freedom each is contained in the blocks labeled "Steering System", "Brake System", and "Power Train." Representative vehicle and tire parameters that must be supplied for a typical simulation run are tabulated in Table 1 for the five passenger vehicle models that were selected in step (2).

The suspension system modeled in VDANL exerts forces on three lumped masses. Two unsprung masses represent the front and rear axles with tires, and one sprung mass represents the vehicle's body. Rather than model each component of the suspension individually, VDANL uses composite characteristics of all components to calculate overall roll dynamics. This method produces less complicated calculations and a significant reduction in data size. The simulation program VDANL also includes an option of using both front and rear anti-roll bars to provide extra auxillary roll stiffness.

The simulation program VDANL uses a comprehensive tire model that includes the effects of road surface interaction and saturation limit. This assures accurate representations of real driving conditions, from low-g to limit lateral maneuvers, and for combined lateral and longitudinal maneuvers (for example, brake-in-a-turn). The program VDANL uses tire parameters defined by the Calspan corporation (cf. Table 1) that contain parameters for cornering stiffness, camber stiffness, lateral and circumferential friction, aligning torque, as well as overturning moment.

Besides the above mentioned modelings, the simulation program VDANL also provides a "closed-loop" driving capability by using the block labeled "Automatic Steer System." This block contains internal algorithms that a human driver uses to generate the required steering, braking, and throttle commands. It can also represent how an autonomous steering system generates the needed steering commands. Furthermore, an "Open" module option provides an interface between a user-supplied "subroutine" and the main program. In this research, we used this option to implement four-wheel-steering control algorithms.

Data predicted by VDANL have been extensively validated via road tests for a wide variety of vehicles and driving conditions.[6-9] Results obtained using the simulation program were found to represent measured vehicle responses quite well for most vehicles and maneuvers.

Selected Production Vehicle Models

Five production passenger vehicle models were selected in this study to represent a fleet of passenger vehicles for the VDTV to "emulate." These represented a wide spectrum in vehicle weight: from "small," "compact," "(mid-sized)" to "full-sized" passenger vehicles. Additionally, these five vehicle models were selected because they span wide ranges in both wheelbase ratio and track width ratio. The wheelbase ratio, the ratio between the vehicle's wheelbase and its center of gravity (e. g.) height ($L/h_{c.g.}$), is strongly related to the amount of weight transfer between the rear and front wheels during acceleration/deceleration maneuvers. Track width ratio, the ratio between the vehicle's halved track width and e.g. height ($tw/2h_{c.g.}$), is strongly related to the amount of weight transfer between the inside and outside wheels during lateral cornering maneuvers. Track width ratio also strongly correlates to the likelihood of vehicle rollover.

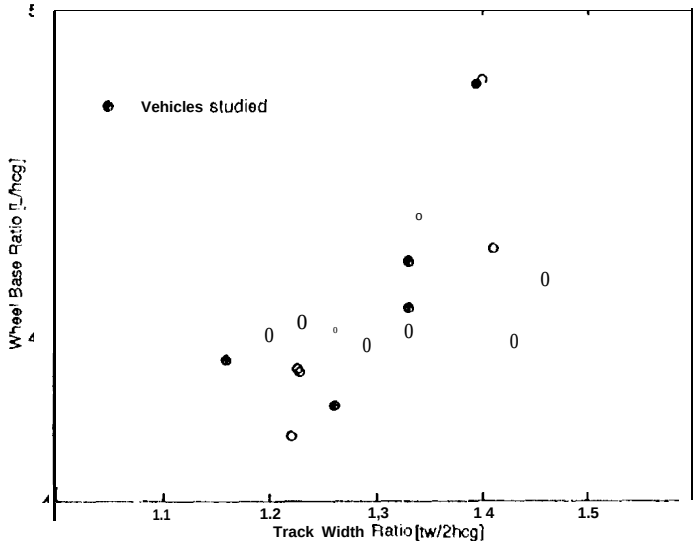

Figure 2: Vehicle's wheelbase ratios versus trackwidth ratios

A plot of wheelbase ratios versus track width ratios for five production vehicles is shown in Figure 2. In that figure, the "0"s denote the wheelbase and track width ratios combinations of production vehicle models with parameter files available from the VI)ANL program. The ". "s represent the five selected passenger vehicle models. Clearly, the selected vehicles span good ranges in both the wheel base ratios and the track width ratios. Estimated values of other vehicle and tire parameters arc tabulated in '1'able 1. See Appendix E of Reference 10 for the estimated values of vehicle and tire parameters that arc not given in '1'able 1.

Steady-state ant] Transient Lateral Response Characteristics of Passenger Vehicles

Using the simulation program VIDANL, and estimates of vehicle and tire parameters given in 'J'able 1, three steady-state and transient lateral response performance metrics of the five selected passenger vehicles were computed. Results are given in the following sections.

The steady-state handling quality of a vehicle can be characterized by its understeer coefficient (K_u, in deg/g). The understeer coefficient, defined in sub-section 9.4.7 of Reference 11, can be understood using the following steady-sta.tc cornering equilibrium equation:

$$\delta_T = \delta_{SW}/N_S = \overbrace{57.3L/R}^{Ackerman\ angle} - K_u a_y , \qquad (1)$$

where,

δ_T = tire angle (deg),
δ_{SW} = steering wheel angle (deg),
N_S = steering ratio (-),
L = wheel base (in),
R = turning radius (m),
K_u = understeer coefficient (deg/g),
a_y = lateral acceleration at vehicle's e.g. (g).

From this equation, the understeer coefficient of a vehicle can be determined with a "turn circle" maneuver. In this maneuver, the forward speed of the vehicle is kept constant at, for example, 80 km/h. The steering; wheel angle is increased slowly at an uniform rate of about 5 deg/sec until the limit lateral acceleration of the vehicle is reached. A cross plot between the latcra] acceleration of the vehicle's c.g. on the X-axis and the steering wheel angle on the Y-axis can then be generated. From this plot, the understeer coefficient is determined as follows:

$$K_u = -\frac{1}{N_S}\frac{\partial \delta_{SW}}{\partial a_y} - 57.3\frac{g\,L}{U^2} . \qquad (2)$$

The first term on the right hand side of equation (2) can be derived from the instantaneous slope of the a_y versus δ_{SW} plot at a given lateral acceleration. The variable "U" in the second term represents the forward speed of the vehicle. That term can be easily computed if we know the wheelbase of the vehicle as well as the speed at which that simulation run was performed. Results obtained from these turn circle maneuvers are given in two cross plots: vehicle's lateral acceleration versus the steering wheel angle (Figure 3), and lateral acceleration versus the understeer coefficient (Figure 4), for the five selected passenger vehicles. From Figure 4, we note that the understeer coefficients of these vehicles remain unchanged when the lateral acceleration of the vehicle is lower than about 0.3 g. However, these understeer coefficients increase drastically as their respect i ve li n nit lateral acceleration levels are approached. These results arc fairly representative for most passenger vehicles.

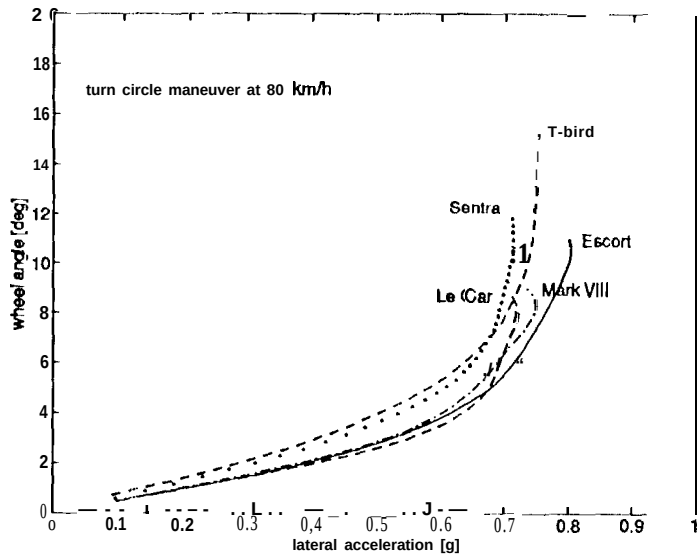

Figure 3: Turn circle maneuver, steering wheel angle versus lateral acceleration

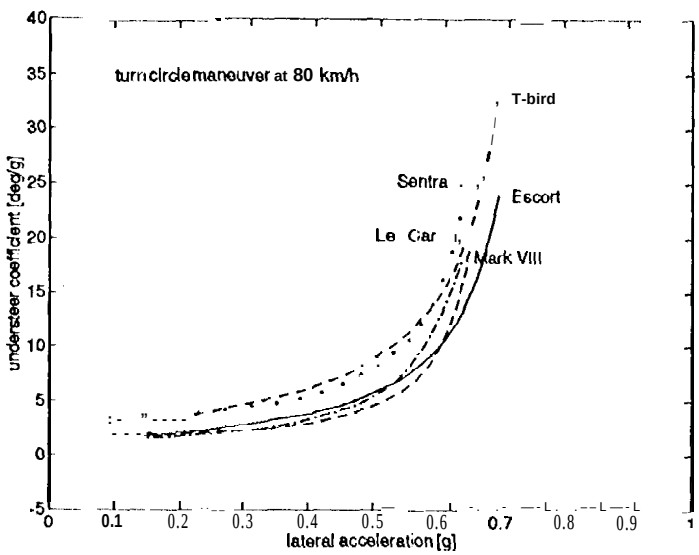

Figure 4: Turn circle maneuver, understeer coefficient versus lateral acceleration

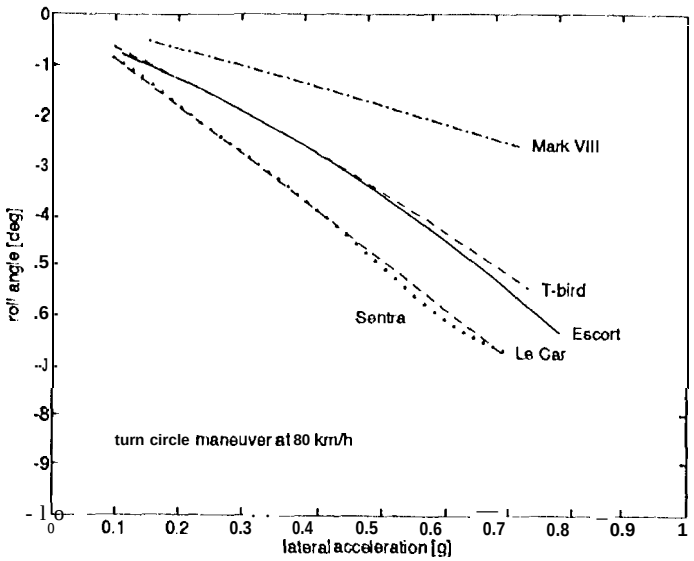

Figure 5: Turn circle maneuver, roll angle versus lateral acceleration

Another performance metric commonly used to characterize the steacly-state vehicle handling quality of a vehicle is its control sensitivity (in g/deg). The control sensitivity of a vehicle at a given forward speed is also known as its steering sensitivity or lateral acceleration gain. In equation (1), the vehicle control sensitivity is given by a_y/δ_{SW}. The relation between the vehicle's control sensitivity and its understeer coefficient is given by:

$$\frac{a_y}{\delta_{SW}} = \frac{1}{N_S}\left[\, K_u + 57.3\frac{gL}{U^2} \,\right]^{-1}. \qquad (3)$$

Since the vehicle's control sensitivity can be computed using the understeer coefficient, only the understeer coefficient is used in this study.

The roll gradient of a vehicle can also be determined using data obtained from the turn circle maneuver. A vehicle's roll gradient, defined in sub-section 9.4.19 of Reference 11, can be determined from a cross plot between the lateral acceleration of the vehicle's e.g. and the vehicle's roll angle. Results obtained for the five passenger vehicles are depicted in Figure 5 wherein we note that the roll gradients of full-size vehicles tend to be small, while the reverse is true for small and compact vehicles.

The transient lateral response characteristics of the vehicles are compared using the "90% rise

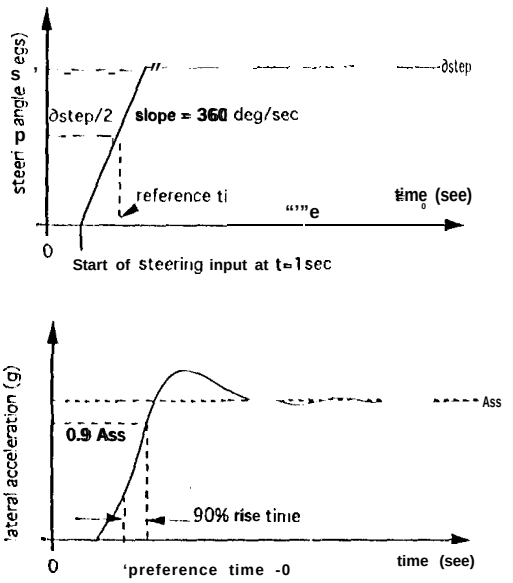

Figure 6: Steering wheel angle and vehicle's lateral acceleration during a J-turn maneuver

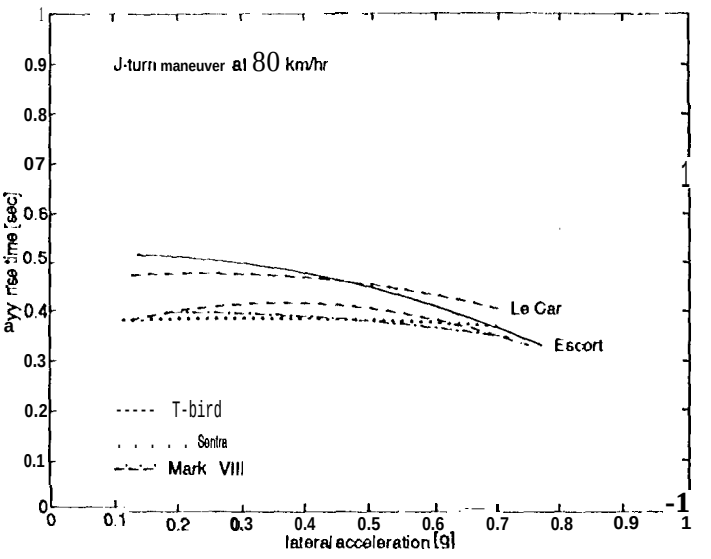

Figure 7: J-turn maneuver, 90% rise time versus lateral acceleration

times" of their lateral acceleration responses. The 90% rise time is a measure of the vehicle's "speed of response" when it is subjected to a "step" steering wheel command. Since a true "step') is physically impossible, the steering command is ramped to its steady-state value at an uniform rate of 360 degrees per second. The resultant maneuver is commonly called a J-turn maneuver. The 90% rise time is defined as the time it takes the vehicle's lateral acceleration to reach 90% of its steady-state value, as measured from the time the steering command reaches 50% of its steady-state value. See Figure 6 and Reference 12 for further details. Plots of the 90% rise time versus the vehicle's lateral acceleration, for the five selected passenger vehicles are depicted in Figure 7.

The speed of lateral response of a vehicle can also be measured using frequency-domain performance metrics such as the vehicle's lateral acceleration -3 dB bandwidth (in Hz). This is the frequency at which the magnitude of the transfer function, from the steering wheel to the vehicle's lateral acceleration, has dropped below 70.7% of its steady-state value. Again, there is a strong correlation between the vehicle's 90% rise time and its lateral acceleration bandwidth. For the 1989 Escort, that correlation is depicted in Figure 8: the larger the bandwidth, the smaller the 90% rise time. A linear approximation between

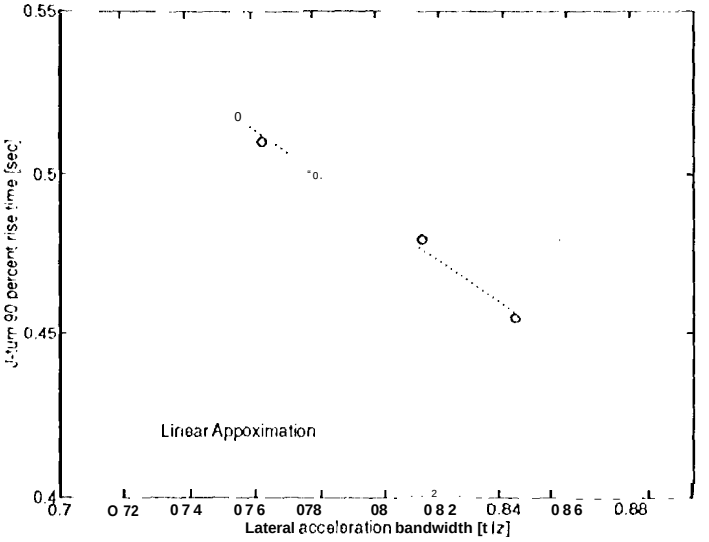

Figure 8: Correlation between vehicle bandwidth and 90% rise time

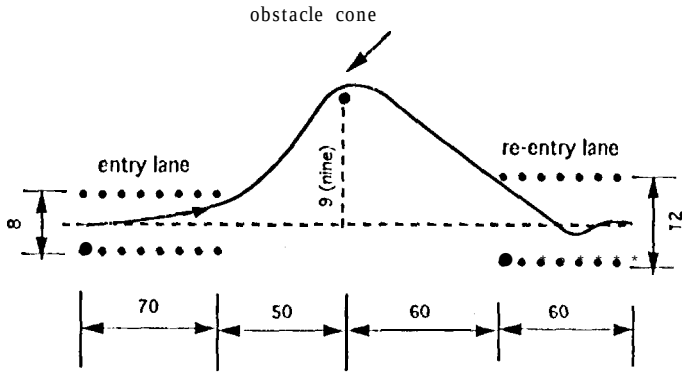

(Not to scale. **All dimensions are in feet)**

Figure 9: Consumers Union obstacle avoidance course

the bandwidth arid rise time is given by:

$$t_{rise} \approx 1.0381 - 0.6888 \times BW . \qquad (4)$$

Here, BW is the vehicle's lateral acceleration bandwidth in Hz, and t_{rise} is the vehicle's J-turn 90% rise time in seconds. Since the lateral acceleration bandwidth is closely correlated with the 90% rise time, only the rise time is used in our Study.

The Consumers Union obstacle avoidance course, depicted in Figure 9, was used to objectively evaluate the handling quality of passenger vehicles during emergency double lane change maneuvers. Details of this obstacle avoidance course arc defined in Reference 13. The maximum speed that a passenger vehicle can successfully complete the double lane change maneuver is denoted by U_{max}. The magnitude of U_{max}, in km/hr, is another lateral response performance metric used in our study.

Selected Baseline Vehicle

For the purpose of dynamics analyses, the 1989 Ford Escort was selected as the baseline variable dynamic testbed vehicle. The following modifications arc made to the production model to account for the added weights of the data acquisition system, four wheel steering actuator mechanism, and others:

- Sprung mass and moment of inertia of the production Escort were each increased by 28% However, these! inertia properties were increased without altering the longitudinal, lateral, and vertical positions of the vehicle's overall e.g. location.

- Spring rates and damper rates of the production vehicle's suspension were each increased by 28%. Since the vehicle sprung mass was increased by 28%, there was no change in either the frequency or damping ratio of the vehicle's heave mode.

- Torsional stiffness of the front anti-roll bar of the production Escort was increased by 28% (in magnitude). The production]) Escort has no rear anti-roll bar.

- "l,arger" tires were selected for the modified Escort. The tire model used is 1'195/75Rl 4.

With these modifications, the weight and moment of inertia of the "compact" Escort were now midway between those of "compact" and "mid-sized" vehicles. It was judged that such a modified Escort could better emulate the lateral response characteristics of both the "small" and "compact" production vehicles, that have higher accident statistics. If a mid-sized vehicle had been selected instead as the baseline vehicle, the added weights would have caused its weight to approach that of a 'Lfull-size" vehicle. This heavier baseline vehicle might not have been able to emulate the lateral response characteristics of both the "small" and "compact" vehicles as well.

Sensitivity Analyses

Two types of sensitivity analyses were performed to assess the degree that selected vehicle performance metrics could be influenced by two vehicle parameters: effects of (I) the torsional stiffnessess of the front and rear anti-roll bars on the vehicle's roll gradient, and (2) the damping rates of the suspension shock absorbers on the 90% rise time of the vehicle in J-turn maneuvers.

Five anti-roll bar configurations used in this study arc depicted in Figure 10. In that figure,

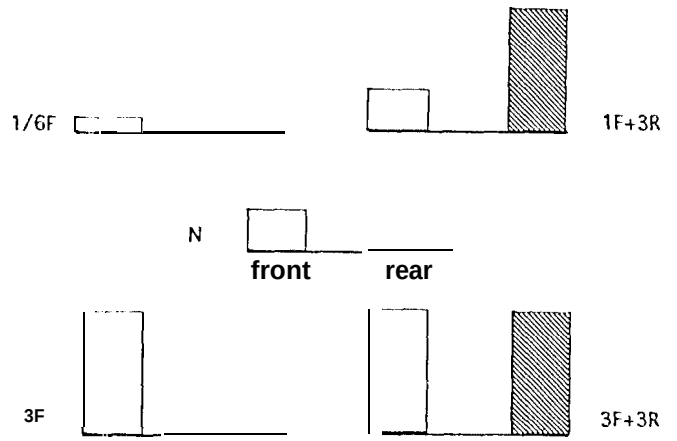

Figure 10: Anti-roll bar stiffness configurations used in a sensitivity analysis

"N" denotes for the "nominal" anti-roll bar configuration of the baseline VDTV: stiffnesses of the front and rear anti-roll bars are -288.6 and O Nm/deg, respectively (the baseline VDTV does not have a rear anti-roll bar). The stiffnesses of all the other anti-roll bar configuration variants are multiples of the nominal front anti-roll bar stiffness. For example, the front and rear anti-roll bar stiffnesses of the configuration] labeled "1F-| 3]{," are -288.6 and -865.8 Nm/deg, respectively.

Plots of steering wheel angle versus the vehicle's lateral acceleration obtained in turn circle maneuvers, for the five anti-roll bar configurations, are compared in Figure 11. Plots that compare the vehicle's understeer coefficient, roll gradient, and 90% rise time in a J-turn maneuver are given in Figures 12, 13, and 14, respectively. From Figure 12, we observe:

- For low-g (below 0.3 g) maneuvers, the anti-roll bars' stiffnesses have very little effect on the vehicle's understeer coefficient.

- At high-g conditions, the anti-roll bars' stiffnesses have the following influences on the vehicle's understeer coefficient:

  understeer coefficient is increased by an increase in the front anti-roll bar stiffness. See results obtained for the "3F" configuration.

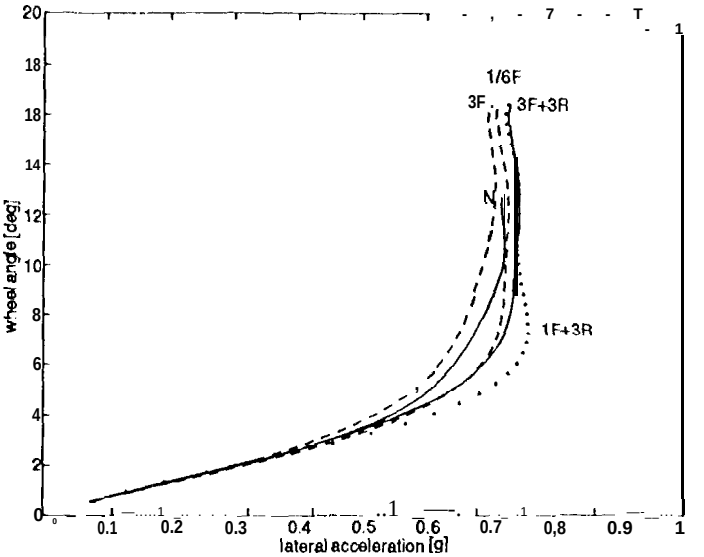

Figure 11: Turn circle maneuver results for five anti-roll bar configurations

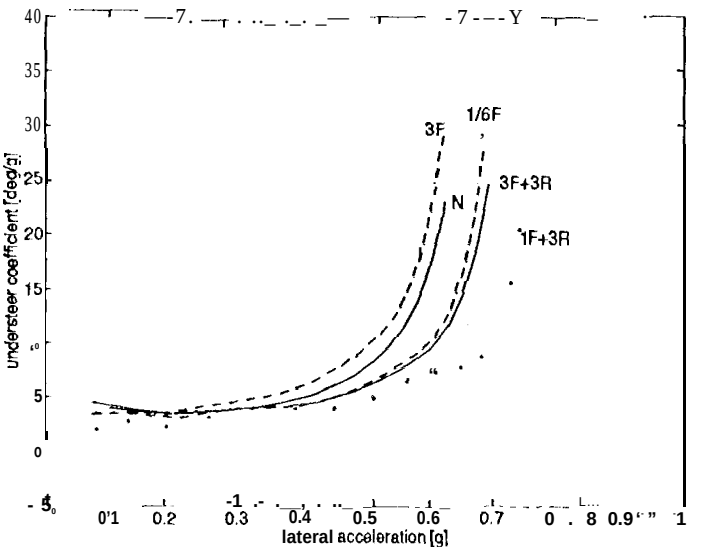

Figure 12: Understeer coefficient results for five anti-roll bar configurations

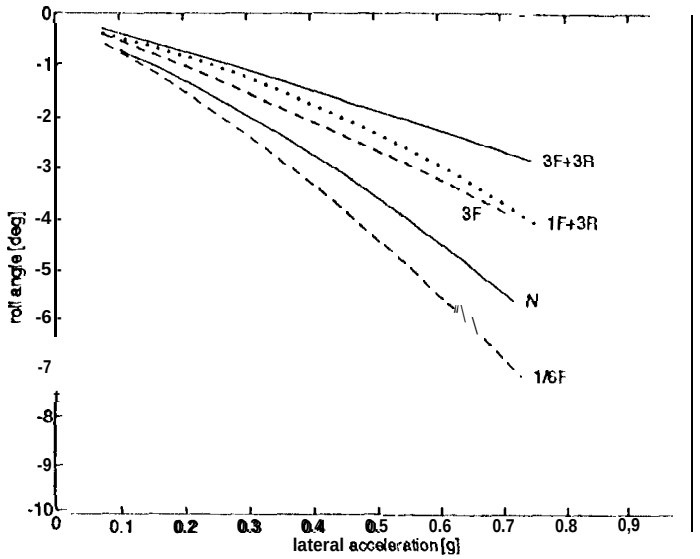

Figure 13: Vehicle roll gradient results for five anti-roll bar configurations

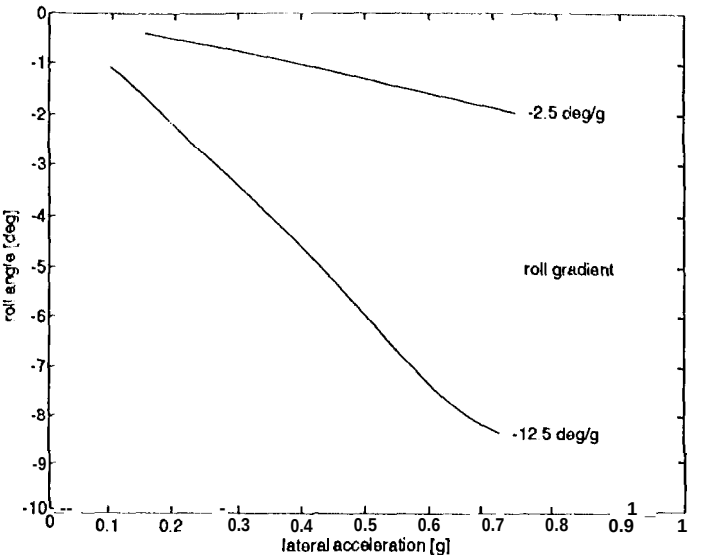

Figure 14: Emulation range of an active anti-roll bar controlled system

understeer coefficient is decreased by an increase in the rear anti-roll bar stiffness. See results obtained for the "1 F+3R" configuration. Alternatively, the vehicle's understeer coefficient can be decreased by decreasing the front anti-roll bar stiffness. See results obtained for the "$\frac{1}{6}$F" configuration.

From Figure 13, we conclude that the stiffnesses of the anti-roll bars have a dominant influence on the vehicle's roll gradient. The larger the magnitude of the total anti-roll bar stiffness (sum of both the front and rear anti-roll bar stiffnesses), the smaller is the vehicle's roll gradient. Hence, the roll gradient for the "3F+3R" configuration is the smallest among the five configurations studied. Hence, changing the stiffnesses of the vehicle's anti-roll bars (either mechanically or by using active anti-roll bar controlled systems) is an effective way to alter the vehicle's roll gradient. The alternative of using a fully active suspension system to control the vehicle roll gradient is likely to be more expensive.

The specified emulation range of the VDTV's roll gradient, depicted in Figure 14, is obtained using results depicted in Figure 13: (a) the lower limit is obtained by reducing 25% from the roll gradient of the "3F+3R" configuration, and (b) the upper limit is obtained by adding 25% to the roll gradient of the "$\frac{1}{6}$F" configuration. This specified emulation range of the vehicle's roll gradient also appeared in Section 7.1.2 of Reference 14. Note also that the upper and lower roll gradient limits depicted in Figure 13 completely envelop the a_y versus roll angle plots of the five passenger vehicles given in Figure 5.

The effects that anti-roll bar stiffnesses have on the 90% rise time in J-turn maneuvers are less obvious. However, the following trends are observed in Figure 15:

- vehicle becomes more responsive (with a smaller J-turn 90% rise time) if the stiffness of the front anti-roll bar is increased. See results obtained for the "3F" configuration.
- vehicle becomes less responsive (with a larger J-turn 90% rise time) if the stiffness of the front anti-roll bar is decreased. See results obtained for the "$\frac{1}{6}$F" configuration.
- vehicle also becomes less responsive (with a larger J-turn 90% rise time) if the stiffness of the rear anti-roll bar is increased. See results obtained for the "1 F+3R" configuration.

The objective of the second set of senstivity analyses was to assess to what degree the damping rates of the vehicle suspension influence the

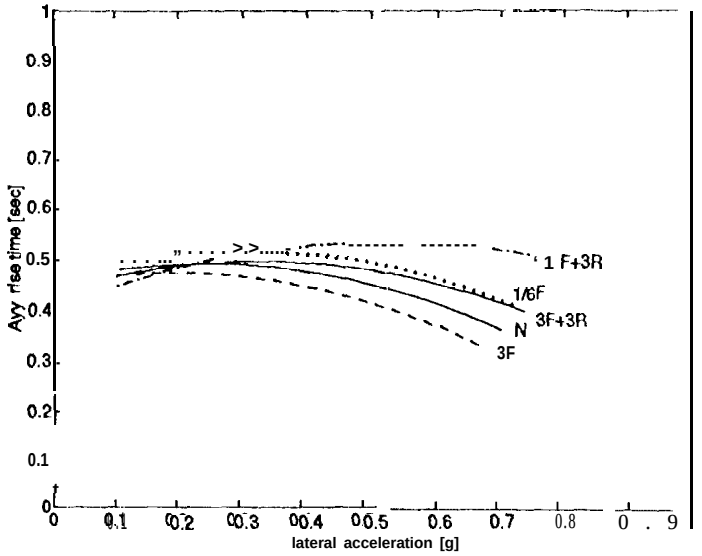

Figure 1 5: Rise time results for five anti-roll bar configurations

vehicle's J-turn 90% rise time. This analysis was performed for the Jet I'repulsion Laboratory by Systems Technology Incorporated. Results obtained arc summarized in the following two paragraphs while the details are given in Reference 15.

Three sets of damper rates were used in the sensitivity analyses. The "hardest" damping rates arc: at a piston speed of 75 cIn/see, the damping forces arc 3400 and 900 Newtons in extension and compression, respectivel y. The "softest" damping rates arc: at a piston speed of 75 cln/see, the damping forces arc 1200 and 670 Newtons in extension and compression, respectively. The nominal damping forces arc between those of the "hardest," and "softest" dampers. These damping rates arc identical to those specified in sub-section 4.3.8 of Reference 14.

Using the above mentioned damping rates, the 90% rise times of a vehicle in a 80 km/hr 0.22 g J-turn maneuver were determined using VI) ANL. The 90% rise times obtained were 0.43, 0.51, and 0.49 seconds for the "softest, " "nominal," and "hardest" damping rates, respectively. Differences among these rise times are quite small. Considering the accuracy of the VDANL simulation program, wc concluded that suspension damping rates do not significantly influence the speed of response of a vehicle in cornering maneuvers.

Four-Wheel-Steering Control Algorithms

The lateral dynamics of a vehicle can be substantially altered by steering its rear wheels in conjunction with the front wheels. For example, the control sensitivity of a four-wheel-steering vehicle at a given forward speed can be increased/decreased by steering the rear wheels out-of-pllasc/ill-phase respectively with the front wheels. Additionally, the transient lateral response characteristics of the vehicle can also be manipulated via carefully designed rear steering algorithms.

Both open-loop and closed-loop 4WS algorithms have been proposed and used in vehicle research.'[6-19] Closed-loop 4WS algorithms usc selected vehicle measurements (for example, vehicle's yaw rate) as well as the driver's steering command to control the rear steering actuator. On the other hand, open-loop algorithms do not feedback any vehicle measurements. The open-loop and closed-loop control algorithms described in the following sub-section arc taken from Reference 19. They arc given here to illustrate the flexibility available to alter the lateral response characteristics of a VDTV via four-wheel-steering algorithms.

- 4WSN Algorithm: This is an open-loop algorithm first suggested by Nissan Motor Company. Using a vehicle model, a speed-dependent ratio between the rear and front wheels is computed in order to achieve zero steady-sta,tc side velocity:

$$\delta_{rc}/\delta_{fc} = K_N(U). \qquad (5)$$

Here, δ_{fc} equals the driver steering wheel command divided by the steering ratio. The command to the rear steering actuator is given by δ_{rc}. The variable U is the forward speed of the vehicle. The function K_N is the "Nissan" ratio. At low speeds, the rear wheels arc steered out-of-phase with the front wheels (i.e., K_N is negative) to enhance the vehicle maneuverability. At high speeds, the rear wheels arc steered in-phase with the front

wheels (i.e., K_N is positive) to enhance the vehicle lateral stability. 1 lowever, the lateral fore.cs generated by both the front and rear wheels counteract one another, and the response time of the vehicle's yaw rate may deteriorate. To overcome this problem, we delay the steering of the rear wheel by τ_D seconds:[17]

$$\delta_{rc}(t) = K_N(U)\,\delta_{fc}(t - \tau_D)\,. \qquad (6)$$

The delay time τ_D is on the order of 0.1 seconds. The parameters K_N and τ_D in this "delayed" Nissan algorithm can be used to alter the steady-state and transient response characteristics of the vehicle, respectively.[17] Numerous other open-loop 4WS algorithms have also been suggested. See, for example, Reference 18. However, open-loop algorithms Were not used in our study.

- 4WSY Algorithm: This is a simple closed-loop algorithm with feed-forward of the front steering command and feedback of the vehicle's yaw-rate:

$$\delta_{rc} = K_1(U)\,\delta_{fc} - K_2(U)\,r\,. \qquad (7)$$

1 lere, the variable δ_{fc} was defined in connection with the 4WSN algorithm. The variable r is the filtered yaw rate of the vehicle. This closed-loop 4 WS algorithm, depicted in Figure 16, was the main focus of our study.

In equation (7), the feed-forward gain K_1 (U) chiefly alters the vehicle's steady-state responses. On the other hand, the feedback gain $K_2(U)$ affects both the steady-st,atc and transient characteristics of the vehicle. Both parameters must be selected with care. The rear steering angle increases monotonically with the magnitude of K_1. Since the maximum rear steering actuator excursion is typically bounded (say, not more than 10 degrees), the magnitude of K_1 must be selected within this physical constraint. On the other hand, feeding back the vehicle's yaw rate can

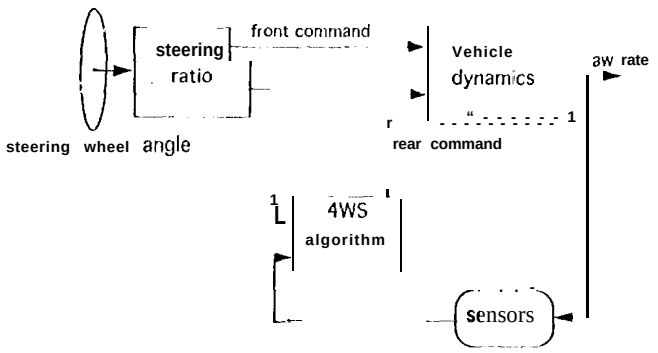

Figure 1 6: Fou r wheel steering cent rolled configuration

degrade the closed-loop stability of a four-wheel-steering vehicle. Care must be exercised to ensure that the damping ratio of the vehicle's yaw mode is always above a preselected minimum level. Appropriately selected, these control parameters allow us to vary the lateral dynamics of the VDTV so that it emulates the response characteristics of a broad range of vehicles.

For sim plicity, the control parameters K_1 and K_2 are not made functions of the vehicle's forward speed in our study. In practice, they can be made functions of both the vehicle's forward velocity and other vehicle measurements such as its lateral acceleration. Other closed-loo]) 4wS algorithms have also been proposed in the literature.*[8-19]

Plots of steering wheel angle versus the vehicle's lateral acceleration obtained from turn circle maneuvers, for four combinations of control parameters (K_1, K_2) arc compared in Figure 17. In that figure, 4WS control algorithms that steered the front and rear wheels "in-phase" have positive K_1, and arc denoted by "11" and "12". 011 the other hand, 4WS control algorithms that steered the front and rear wheels "out-of- phase" have negative K_1, and arc denoted by "O1" and "O2". Plots that compare the understeer coefficients of the nominal two-wheel-steering vehicle, and the "12" and "02'" four-wheel-steering vehicles are

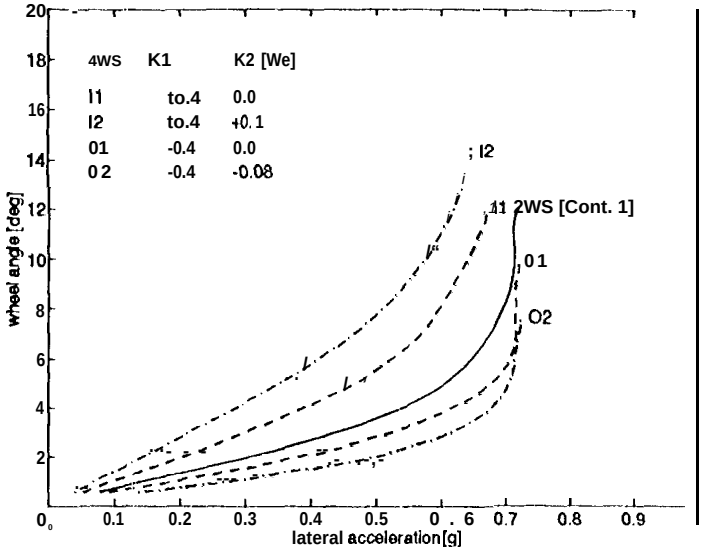

Figure 17: Turn cicrle maneuver results obtained with 4WS VDTV [Configuration I]

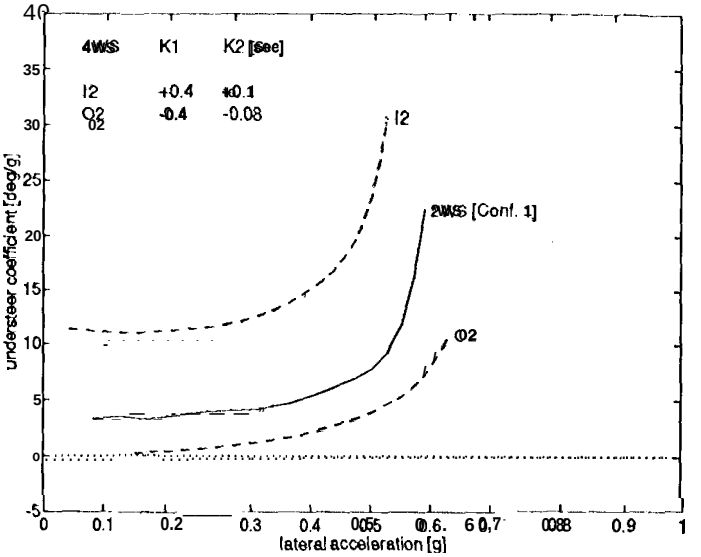

Figure 18: Understeer coefficient results obtained with **4WS** VDTV [Configuration I]

shown in Figure 18. For clarity, results obtained for the "11" and "01" four-wheel-steerillg vehicles are omitted in that figure. The following observations can be made from Figure 18:

- the understeer coefficient of the four-wheel-steering vehicle is increased by steering the rear wheels in-phase with the front wheels, and can be further increased by having a negative yaw rate feedback (with positive K_2).
- the understeer coefficient of the four-wheel-steering vehicle is decreased by steering the rear wheels out-of-phase with the front wheels, and can be further decreased by having a positive yaw rate feedback (with negative K_2).

In Figures **17** and 18, the two-wheel-steering vehicle is denoted by "2WS [Configuration 1]. " Results obtained for a second two-wheel-steering vehicle, denoted by "2WS [Configuration 11]" are given in Figures 19 and **20.** The main difference between these two configurations is: all four tires used in the "Configuration 1" are 1)195/751{.14 tires (that are used by the Toyota Van in Reference 1 o). For "Configuration 1 I", the two front tires of "Configuration I" are replaced by two 1'195/751{14 tires (that are used by the Chevrolet S10 in Reference 10).

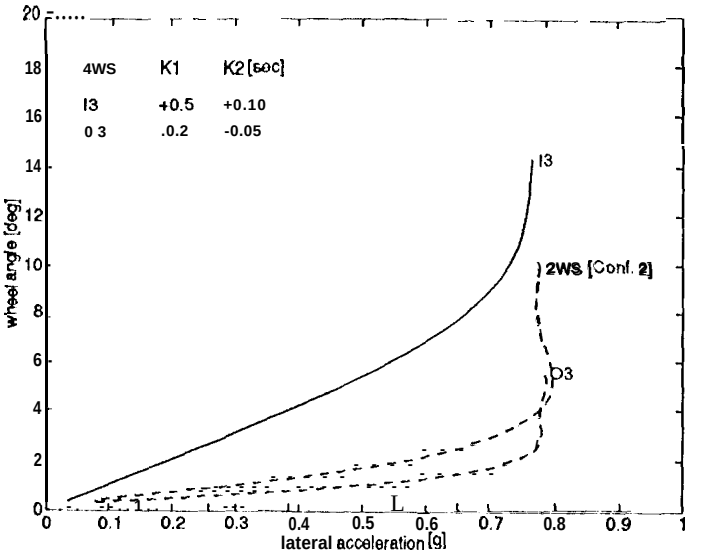

Figure 19: Turn cicrle maneuver results obtained with 4WSVDTV [Configuration 11]

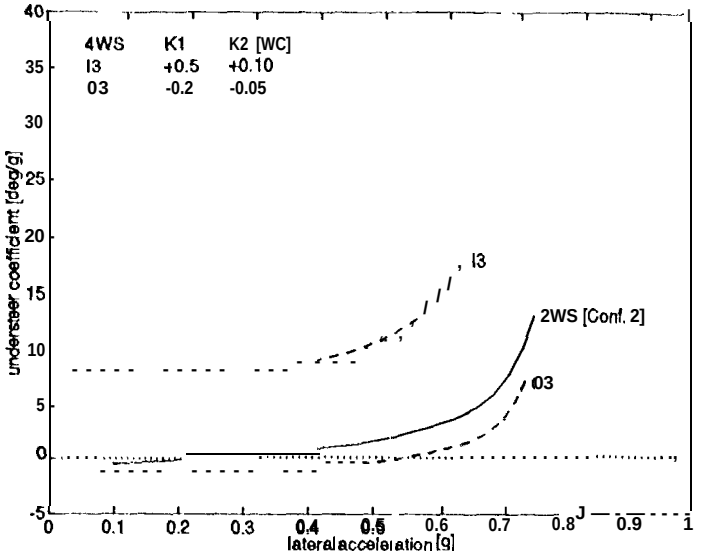

Figure 20: Understeer coefficient results obtained with 4WS VDTV [Configuration 11]

Turn circle maneuver results obtained with the second two-wheel-st,ccring vehicle and its four-wllcel-stew.ring derivatives are given in Figures 19 and 20. In Figure 20, the second two-wheel-steering vehicle controlled by the '(03'" 4WS algorithm can generate negative understeer coeffi - cient (i .e., oversteer). The emulation range of the VI)'I "V's understeer coefficient, estimated using results given in Figures 1$ and 20, is depicted in Figure 21. The upper bound in that figure was obtained by adding 25% to the result obtained for the "I2" four-wllecl-steering vehicle (see Figure 18). The lower bound in that figure was obtained by subtracting **2.5** deg/g from result obtained for the **"03'"** four-wheel-steering vehicle (see Figure 20).

The effects that 4WS control algorithms have on the vehicle's 90% rise time in J-turn maneuvers arc fairly significant. The following observations can be made from Figure 22:

- vehicle becomes more responsive (with a smaller J-turn 90% rise time) if the front and rear tires arc steered in-phase and with a negative yaw rate feedback (positive K_2). SCc results obtained for the "13" four-wheel-steering vehicle.

- vehicle becomes even more responsive if the stiffness of the front anti-roll bar is increased.

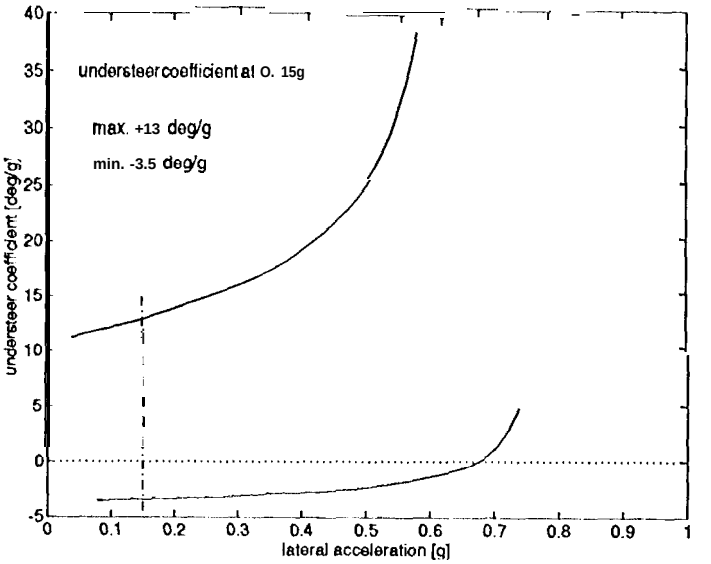

Figure **21:** Emulation range of the VDTV understeer coefficient

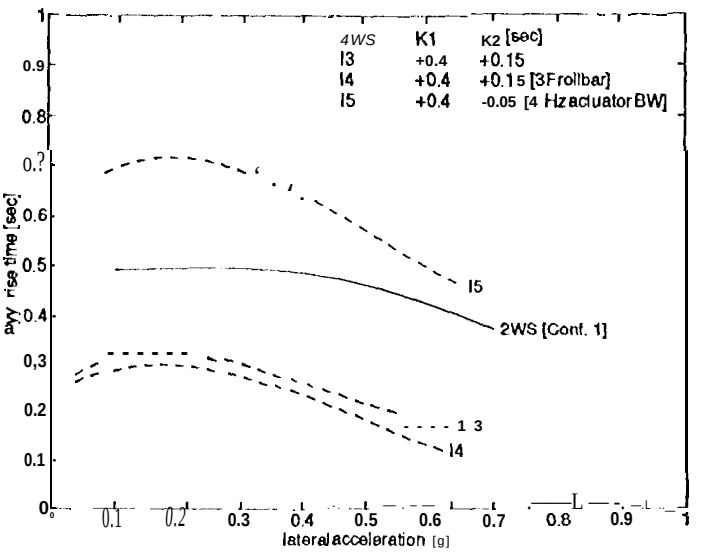

Figure **22:** Rise time results obtained with a 4WS VDTV

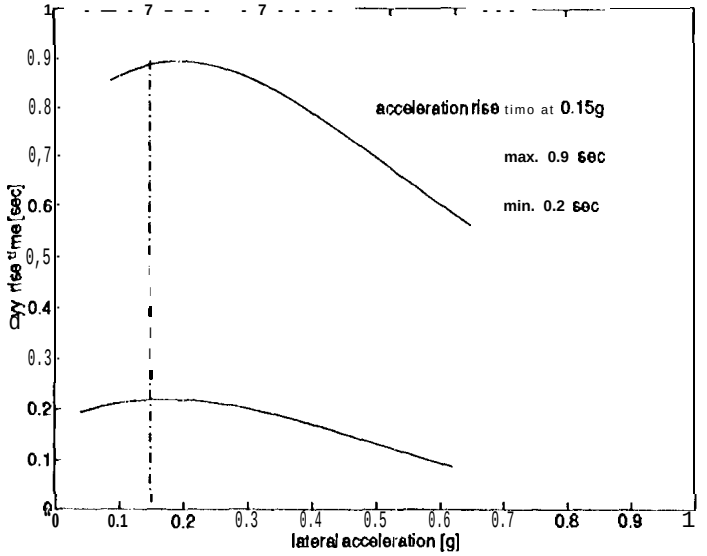

Figure 23: Emulation range of the VDTV J turn 90% rise time

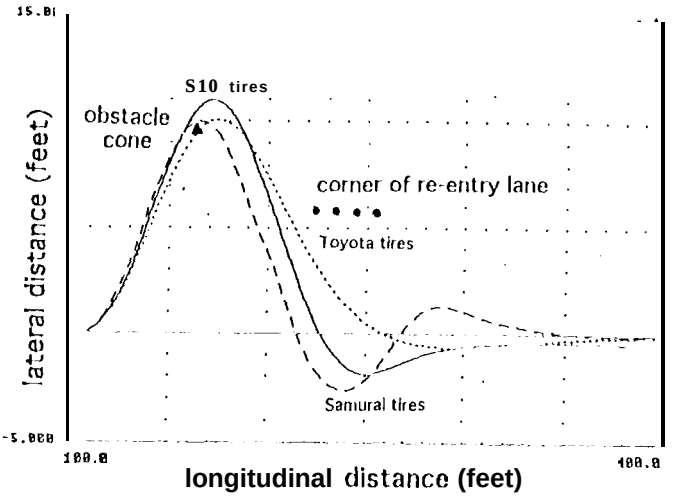

Figure 24: obstacle avoidance lane change maneuver results

See results obtained for "14" four-wheel-steering vehicle.

- vehicle becomes less responsive (with a larger J-turn 90% rise time) if the front and rear tires are steered in-phase and with a positive yaw rate feedback (negative K_2), as well as using a steering actuator with a lower bandwidth of 4 Hertz (the nominal bandwidth of the steering actuator is on the order of I O Hz). See results obtained for the "15" four-wheel-steering vehicle.

The emulation range for the VD TV's J-turn 90% rise time is depicted in Figure 23. The upper and lower bounds in that figure are obtained by increasing and decreasing, respectively, 25'% of results obtained by the "15" and "14" four-wheel-steering vehicles that are depicted in Figure **22.**

Results obtained from the Consumers Union Obstacle Course

Consumers Union obstacle avoidance course, depicted in Figure 9, was used to objectively evaluate the handling qualities of passenger vehicles during emergency double lane change maneuvers. Details of this obstacle avoidance course are defined in Reference 13. The VDANL closed-loop crash avoidance option was used to determine the maximum speed at which the baseline VDTV (with 1'195/751{14 Toyota Van tires) can successfully complete this double lane change maneuver. This analytical simulation was then repeated on two other VDTV variants: the first has 1'195/751tl 4 Chevrolet S1 O tires and the second has }'205/701{.15 Samurai tires. The maximum speed was found using the Samurai tires, and was 52.7 km/hr. In Section **3.5.2.3** of Reference 14, we specified that the VDTV shall be able to successfully negotiate the Consu mers Union obstacle course at a]] speeds below 55 km/hr.

Figure 24 displays the lateral versus longitudinal positions for the crash avoidance double lane change maneuver of the three VDTV variants with different tire models. As shown ill that figure, all three VDTV variants can clear the corner of the re-entry lane, but only the variants with the S1O and Samurai tires can clear the obstacle cone. The VDTV with the Samurai tires is most "aggressive>' because it can get back to the centerline of the re-entry lane in the shortest longitudinal distance. However, the vehicle trajectory beyond that "crossover" point is quite oscillatory. On the other hand, the vehicle trajectory obtained with the S10 tires, both before arid after the crossover point is better damped. Time histories of the steering wheel angle, vehicle's latera acceleration and sideslip angle, as well as tire

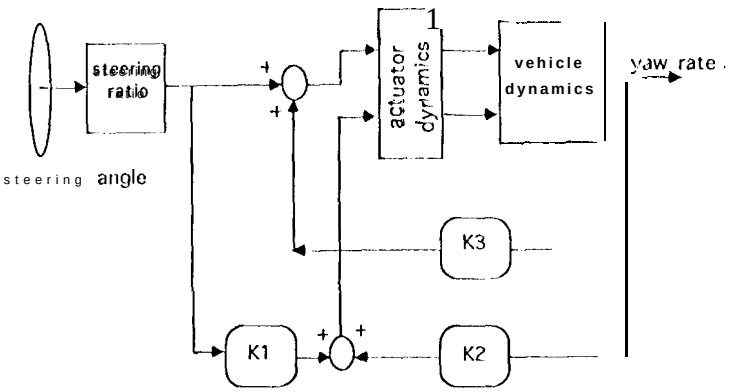

Figure 25: A combined four-wheel-steering and steer-by-wire control architecture

forces are given in Reference 15.

Concluding Remarks

A Variable Dynamic Testbed Vehicle concept has been proposed as a tool to perform driving-related human factors research. The goal of this study was to analytically investigate to what degree a VDTV with four-wheel-steering can emulate the lateral dynamics of a broad range of vehicle models. Using a selected colnl)act-sized automobile as a baseline, our study indicated this vehicle can be controlled to emulate the latcra] response characteristics (including the vehicle's understeer coefficient and the 90% lateral acceleration rise time in a J-turn maneuver) of a flee.t of production vehicles, from low to high lateral acceleration conditions. Also, the roll gradient of the baselined vehicle can be altered via changes made to the torsional stiffnesses of the front arid/or rear anti-roll bars to emulate the roll stiffnesses of a fleet of production vehicles.

The levels of emulation can potentially be improved if the VDTV has both the four-wheel-steering and steer-by-wire features depicted in Figure 25. With this steering configuration, the controller architecture given in (7) becomes:

$$\delta_{rc} = K_1(U)\delta_{fc} + K_2(U)r, \qquad (8)$$

$$\delta_{fc} = \delta_{fc} + K_3(U)r. \qquad (9)$$

Here, the variables δ_{fc} and r were defined in connection with the 4WSY control algorithm. Front and rear steering commands are given by δ_{fc} and δ_{rc}, respectively. The added emulation benefits that one can derive with this controller adlitxcture are not confirmed in this study, but experimental results obtained from a vehicle fitted with a similar steering system have shown promise.[3] The proposed VDTV, with both the steer-by-wire and four-wheel-steering features,[14] will be an idea] testbed to verify results obtained by the Simulator Vehicle of Reference 3.

Acknowledgments

The research described in this paper was carried out by the Jet Propulsion laboratory, California Institute of Technology. It was sponsored by the National Highway Traffic Safety Administration through an agreement with the National Aeronautics and Space Adminstration. The authors wish to thank their colleagues at Jet Propulsion laboratory, including D. Griffin, M. Koffman, R. Norton, and R. Phen; W. Allen, D. Klyde, and 'J'. Rosenthal at Systems Technology Incorporated, as well as J. Chrstos and R. Garrott at the Vehicle Research and Test Center for many helpful discussions. This research was conducted under the technical direction of L. Emery of the National Highway Traffic Safety Adminstration. All errors are our responsibility.

Disclaimer

The discussion in the text of this paper reflects the opinion and findings of the authors, and not necessarily those of the National Highway Traffic Safety Adminstration.

References

1. Leasure, W. A., Jr., "The NHTSA Collision Avoidance Program," IVHS America Workshop on Collision Avoidance, Reston, Virginia, April 21-22, 1994.

2 McKenna, K. J., "A Variable Response Vehicle - Description and Applications," Joint Automatic Control Conference, Austin, Texas, June 19-21, 1974.

3. Sugasawa, 1"., Irie, N., and Kuroki, J., "Development of A Simulator Vehicle for Conducting Vehicle Dynamics Research ," International Journal of Vehicle Design, Vol. 13, No. 2, pp. 159-167, 1992.

4. Marriott, A., "Variable Dynamic Testbed Vehicle," SAE 950036, 1995.

5. Allen, W., Rosenthal, 'J'., and Szostak, 11., "Steady State and Transient Analysis of Ground Vehicle Handling," SAE 870495, 1987.

6. Allen, W., Szostak, 11., Rosenthal, '1'., and Klyde, 1)., "Field Testing and Computer Simulation Analysis of Ground Vehicle Dynamic Stability," SAE 900127.

7. Bernard, J., et al, "Evaluation of Selected Vehicle Dynamics: Phase II Final Report," MVMA Project: IOWA 9114 -C11302, Iowa State University, College of Engineering, June 1992.

8. Heydinger, G., "Vehicle Dynamic Simulation and Metric Computation for Comparison with Accident Data," NHTSA DOT HS 807828, Final Report, March 1991.

9. Allen, W., Rosenthal, T., Klyde, 1)., Owens, K., and Szostak, 11., "Validation of Ground Vehicle Computer Simulation 1 Developed for Dynamic Stability Analysis," SAE 920054.

10. Allen, W., Szostak, 11., Klyde, D., Rosenthal, 'J'., and Owens, K., "Vehicle Dynamic Stability and Rollover," National Highway Traffic Safety Adminstration, DOT HS 807 956, Final Report, June 1992.

11. SAE Handbook (1992), Volume 4: "On-highway Vehicles and Off-highway Machincry," Vehicle 1 Dynamics Terminology, SA E J670e. Published by SAE, Inc., 400 Commonwealth Drive, Warrendale, PA] 5096-0001.

12. Lee, A. Y., "Emulating the Lateral Dynamic of A Range of Vehicles Using A Four-wheel-steering Vehicle," SAE 950304. See also Sl'-1074, "New Development in Vehicle Dynamics, Simulation, and Suspension Systems," pp. 11-22, 1995.

13. Riley, B. and Robinson, B., "Handling Test on Pour-wl]ccl-drive Multi-purpose Vehicles," Research Report 330, Transportation and Road Research Laboratory, U. K., 1991.

14! Griffin, D. C., "Variable Dynamic Testbed Vehicle (VDTV): Functional Requirements," JPL Publication 1)-13459, April 1996. Published by Jet Propulsion laboratory, 4800 Oak Grove Drive, Pasadena, California 91109-8099.

15< Klyde, 1)., Allen, W., and Rosenthal, T., "VDANL Sensitivity Analysis With A Modified Ford Escort," Working Paper 2544-1, December 18, 1995. Published by Systems Technology, incorporated, 13766 South Hawthorne Blvd., Hawthorne, California 90250-7083.

16. Lee, A. Y., "Vehicle Stability Augmentation Systems Designs for Four Wheel Steering Vehicles," ASME Journal of Dynamical Systems, Measurements and Control, Vol. 112, No. 3, September 1990.

17, Fukunada, Y., Irie, N., Kuroki, J., and Sugasawa, }"., "Improved Handling and Stability Using Four-Wheel-Steering," The 11 th International Conference on Experimental Technical Safety Vehicles, Washington, D. C., May 1987.

18. Takiguchi, 'i'., Yasuda, N., Furutani, S., Kanazawa, H., and Inoue, 11., "Improvement of Vehicle Dynamics by Vehicle-speed-sensing Four-wheel-steering System," SAE 860624, February 1986.

19, Lee, A. Y., "Performance of Four-wheel-steering Vehicles in Lane Change Maneuvers," SAE 950316. See also S1'-1 074, "New Development in Vehicle Dynamics, Simulation, and Suspension Systems," pp. 161-1 ?4, 1995.

Table 1

Estimated Values of Vehicle and Tire Parameters†

Parameter	LeCar	Sentra	Escort	T-bird	Mark V]]]
Class	small	small	compact	Illid-size	full-size
Year	1977	1983	1989	1987	1995
wheel base (m)	2.42	2.39	2,39	2 . 6 5	2.89
mean track width (m)	1.27	1.39	1.41	1.49	1.53
e.g. distance from front axle (m)	0.93	0.84	0.88	1.06	1.18
e.g. height (m)	0.54	0.52	0.56	0.56	0.55
track width ratio	1.18	1.34	1.26	1.33	1.39
wheelbase ratio	4.48	4.60	4.27	4.73	5.25
total weight (kg.wt.)	816	1068	1229	1649	1756
roll inertia (kg-m ^{2})	147.3	217.0	244.1	348.8	716.2
pitch inertia (kg-m^2)	797.7	1101,1	1342.4	2537.4	3500.2
yaw inertia (kg-m^2)	986.5	1315.3	1539.1	2976.1	3627.3
front/rear roll stiffnesses (Nm/deg)	165.1 182.8	393.7 295.3	379.8 379.8	305.4 356.2	329.1 421,8
frollt/rear roll damping (Nms/deg)	15.8 15.0	27.1 17.2	25.3 25.3	34.9 32.5	39.1 42.0
front/rear anti-roll bar stiffness (Nm/deg)	-145.8 -75,0	*0* *0*	-224.8 *0*	-714.8 -l 87.7	-2118 -299.3
steering ratio (-)	*20.8*	16.9	18.2	14.3	13.4
tire model	P145/ SR13	1'155/ SR13	P165/ 80R13	1'215/ 701{14	1'215/ 70R14
Calspan coeff's:					
A_0	1260	2380	0	733	733
A_1	13.20	9.21	15.66	19.50	19.50
A_2	1830	2280	2350	2900	2900
A_3	0.533	0.523	0.530	1.370	1.370
A_4	-31200	-7225	-24450	4420	4420

† 1 Mailed information on these and other vehicle/tire parameters are available in Appendix E of Reference 10.